

MICROVASCULATURE SEGMENTATION OF ARTERIOLES USING DEEP CNN

Y. M. Kassim^{○}, V. B. S. Prasath^{*}, O. V. Glinskii^{†‡}, V. V. Glinsky^{†§}, V. H. Huxley^{‡#}, K. Palaniappan^{*}*

^{*}Computational Imaging and VisAnalysis (CIVA) Lab

Department of Electrical Engineering and Computer Science

[†]Department of Medical Pharmacology and Physiology

[‡]Department of Pathology and Anatomical Sciences

[#]National Center for Gender Physiology

University of Missouri-Columbia, Columbia, MO 65211 USA

[○] Research Service, Harry S. Truman Memorial Veterans Hospital, Columbia, MO 65201 USA

[§]Department of Computer Engineering, Al-Nahrain University, Baghdad, Iraq

ABSTRACT

Segmenting microvascular structures is an important requirement in understanding angioadaptation by which vascular networks remodel their morphological structures. Accurate segmentation for separating microvasculature structures is important in quantifying remodeling process. In this work, we utilize a deep convolutional neural network (CNN) framework for obtaining robust segmentations of microvasculature from epifluorescence microscopy imagery of mice dura mater. Due to the inhomogeneous staining of the microvasculature, different binding properties of vessels under fluorescence dye, uneven contrast and low texture content, traditional vessel segmentation approaches obtain sub-optimal accuracy. We consider a deep CNN for the purpose keeping small vessel segments and handle the challenges posed by epifluorescence microscopy imaging modality. Experimental results on ovariectomized - ovary removed (OVX) - mice dura mater epifluorescence microscopy images show that the proposed modified CNN framework obtains an highest accuracy of 99% and better than other vessel segmentation methods.

Index Terms— epifluorescence microscopy, vessel segmentation, deep learning, convolutional neural networks.

1. INTRODUCTION

Vessel and thin structures segmentation is important in many biomedical image analysis problems such retina, ophthalmology, fundoscopy etc. Many of the feature driven segmentation methods utilize multiscale derivatives, Gaussian filters and feature banks [1, 2, 3, 4], topology and shape features [5], interactive segmentation [6], there are also random forests classifier [7], and regression/classification based approaches [8]. However, unlike the characteristics of the retinal vessels, the diffusive nature of microvasculature boundaries in epifluorescence makes automatic segmentation

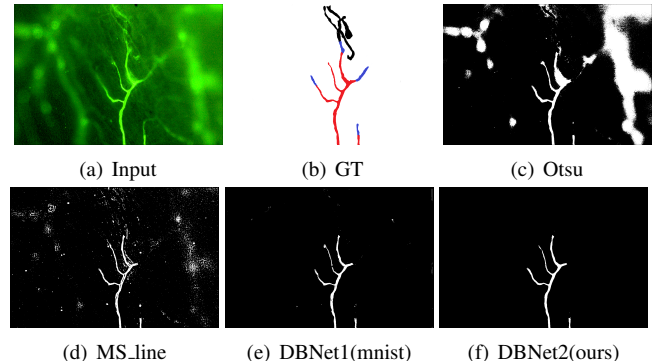


Fig. 1. Our CNN based segmentation framework relies upon predictions of overlapped patches, obtains accurate microvasculature network extraction when compared to experienced physiologists marked ground truth and performs better than other methods. (a) Input image, and (b) manually drawn ground truth (GT) of arterioles represented by red color. Segmentation results obtained by (c) Otsu thresholding, (d) multiscale line detector (MS_line) [11], (e) deep network with 8 layers (DBNet1(mnist)), and (f) Our proposed deep network with 14 layers (DBNet2(ours)).

a challenging problem [9, 10], see Figure 1(a) where the arterioles are surrounded by blurred veins with uneven contrast peculiar to the epifluorescence imaging modality is evident. Thus, there is a need for a robust segmentation approach that can differentiate the microvasculature network from the background.

Deep learning in neural networks are currently popular in computer vision, pattern recognition [12, 13], and showed outstanding performance in solving various biomedical image analysis problems [14, 15, 16]. One of the popular types of deep learning techniques is the convolutional neural network (CNN) which is increasingly applied in various image analysis problems. There have been recent applications of these

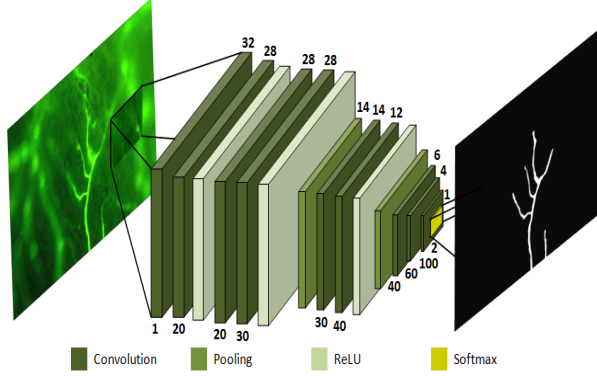


Fig. 2. Architecture of our deep learning CNN configuration employed here for microvasculature segmentation. The approach comprises of 9 convolution layers, 3 ReLU, 2 pooling, 1 softmax layers. The spatial sizes are shown above, and feature maps depth below the corresponding layers.

CNNs to adapt to biomedical applications [17, 18, 19, 20].

In this work, we consider the application of deep learning convolutional networks for epifluorescence microscopy imagery which brings unique challenges due to the inhomogeneous diffusive property of the dyes. These images have drastic illumination changes, blurred vessel boundaries and unlike fundoscopy [18] or multiphoton microscopy [19] contain random color noise. We design a CNN architecture, with the network model built on top of the existing network [21] to suit our epifluorescence microscopy dataset. To the best of our knowledge this work represents the first effort in adapting a CNN architecture to epifluorescence microscopy microvasculature segmentations. Experimental results on a set of ovariectomized (ovary removed, denoted by OVX) mice epifluorescence microscopy images show that the deep learning CNN obtains better accuracy than other popular segmentation approaches [22, 11], and obtains accurate segmentation of microvasculature when compared to ground truth obtained from experienced physiologists, see Figure 1(b-d).

The rest of the paper is organized as follows. Section 2 provides the details of our CNN architecture, and details of the segmentation approach. Section 3 provides experimental results on epifluorescence microscopy with comparisons with other methods. Finally, Section 4 concludes the paper.

2. DEEP CONVOLUTIONAL NEURAL NETWORK FOR MICROVASCULATURE SEGMENTATION

2.1. Overview

In typical classification and pattern recognition problems, convolution neural network (CNN) takes an image as input and produces a probability map as output. It basically performs multiple operations through hidden layers to produce some high level features that can potentially represent the target classes. The important operations that usually occurs are convolution, max pooling and rectified linear units

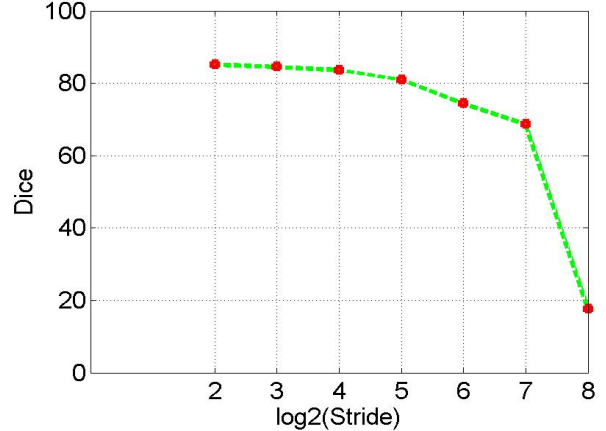


Fig. 3. Dice values versus stride in the studied deep CNN (DBNet2(ours)) for microvasculature segmentation on 20 epifluorescence microscopy images. As the stride gets bigger the number of trained patches is reduced, and the Dice values decrease indicating that the segmentation accuracy is getting lower.

(ReLU). Convolution is responsible for convolving regions with weights represented as filters to produce activation maps with discriminative features. The low level feature maps usually have low level features such as curves or lines, while at the end of the network, high level representation can be achieved. Pooling performs down sampling to collect or combine low-level features in specified area to gain large invariance and sub-region summarization. ReLU is a kind of non-linearity which is useful in solving the gradient vanishing problem caused by the sigmoid function, in addition it produces sparse representation that makes the network fast to learn. Softmax classification is used to discriminate between classes depending upon the probabilities produced from the fully connected layer.

2.2. Network architecture

In our work, we utilized deep CNN for the purpose of microvasculature segmentation from epifluorescence microscopy imagery. Our adapted CNN receives 32×32 patches of the microscopy images, and outputs two classes for microvasculature network as foreground, and other regions as background. This network has been built on top of the existing MatConvNet toolbox [21]. Originally, we tried to adapt a network that has been used for mnist recognition widely (DB-Net1(mnist)), which consists of 4 convolution, 2 pooling and 1 ReLU with input size equal to 28×28 . However, we found from our experiments that this standard network was not deep enough to capture the properties for our complex epifluorescence microscopy imagery. In addition, with 28×28 patches the network could not specify whether the region is a vessel or just an epifluorescence dye leakage.

To obtain better segmentations, we built a new CNN architecture (DBNet2(ours)) which is more deeper with input

Table 1. Effect on overall average Dice values for the number of trained patches in our CNN (DBNet2(ours)) for microvasculature segmentation on 20 epifluorescence images.

Stride	Number of patches	Dice value
256	300	17.73
128	990	68.68
64	3740	74.47
32	14190	81.04
16	55250	83.68
8	221000	84.77
4	880600	85.26

patch size equal to 32×32 . This new configuration consists of 9 convolution layers, 3 ReLU and 2 pooling layers as shown in Figure 2, with the spatial sizes are given above the corresponding layers, and feature maps depth below the layers. The filter size is 5×5 for the first 4 layers, then it is 3×3 for the next 3 layers, with the last two fully connected. Some layers have padding to keep the spatial sizes the same, and others have not; thereby producing output less than the input by $2 \times$ half the filter size. The last softmax layer is to discriminate between the two classes to produce a patch which is either a foreground or background.

2.3. Training and testing

As with any classification and deep learning approaches, the network need to be trained first, and then used that model to test the images. The training phase takes patches from different 10 epifluorescence microscopy images with stride equal to 4 (correspond to 880600 number of patches). Figure 3 shows how the accuracy depends upon the number of trained patches in terms of the Dice values compared to physiologists marked ground truth. When the stride equal to 256, Dice value is lowest at 17.72% since there are only 300 patches used for training. As we continue to decrease the stride from 256 to 4 which obtains 880600 patches, obtains a highest value of 85.26% as shown in table Table 1. We stopped here from decreasing the stride since it requires a huge amount of memory with little difference in increased final accuracy. The training continues for a specific number of epochs which is set at 60.

The training and testing takes about 10 hours, and 20 minutes on a 8-core CPU as it involves a large number of overlapped patches extraction, however we do not use the GPU which can help improve on the computational efficiency. In the testing phase, we used overlapped patches through the network to obtain smooth binary segmentations. In both testing and training phases, the mean value is subtracted from the images to have zero mean and unit variance as preprocessing step. In the training phase, the goal is to let the network learn how to identify a given patch as vessel or non-vessel. We considered each patch as vessel if the corresponding ground truth has 1's in the middle of the patch, i.e. if the four middle pixels in the ground truth are 1, then the corresponding patch

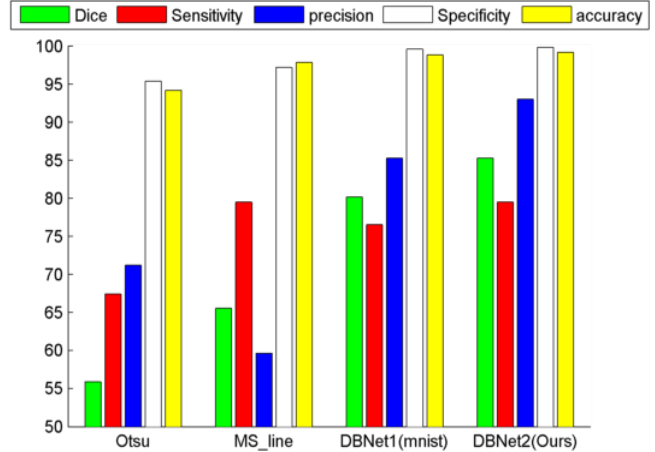


Fig. 4. Comparison of average Dice, sensitivity, precision, specificity, and accuracy for different segmentation methods on a set of 20 epifluorescence OVX microscopy images.

Table 2. Quantitive comparison of segmentation methods on post ovary actomy (OVX) mice dura mater epifluorescence images with global, line detector and two different deep learning networks with different size of input. We show the overall average Dice, sensitivity, precision, specificity, and accuracy values for a set of 20 epifluorescence microscopy images.

Method	Otsu Thresh.	Multiscale Line det.	DBNet (mnist)	DBNet (ours)
Dice	55.91	65.56	80.16	85.26
Sensitivity	67.41	79.48	76.51	79.52
Precision	71.22	59.66	85.24	93.00
Specificity	95.33	97.13	99.54	99.79
Accuracy	94.16	97.80	98.79	99.11

will be labeled as part of a foreground vessel, otherwise, it is considered as background.

3. EXPERIMENTAL RESULTS

3.1. Dataset and setup

The experiments were performed on high resolution epifluorescence images of mice dura mater acquired using a video microscopy system (Laborlux 8 microscope from Leitz Wetzlar, Germany) equipped with 75 watt xenon lamp and QICAM high performance digital CCD camera (Quantitative Imaging Corporation, Burnaby, Canada) at 0.56 micron per pixel resolution. We utilized a set of 20 epifluorescence microscopy images (1360×1036 pixels) of ovariectomized (OVX) mice consisting of 10 ER β -wild type (WT), another 10 from ER β -knock-out (KO). These particular images were selected by three experienced physiologists in order to quantify the difference between ovary intact versus ovary removed in both wild type and knock-out. Further, they were selected to contain a wide differentiability in terms of the image details. In this work, we concentrate on the segmentation accuracy obtained by different methods and show that the our

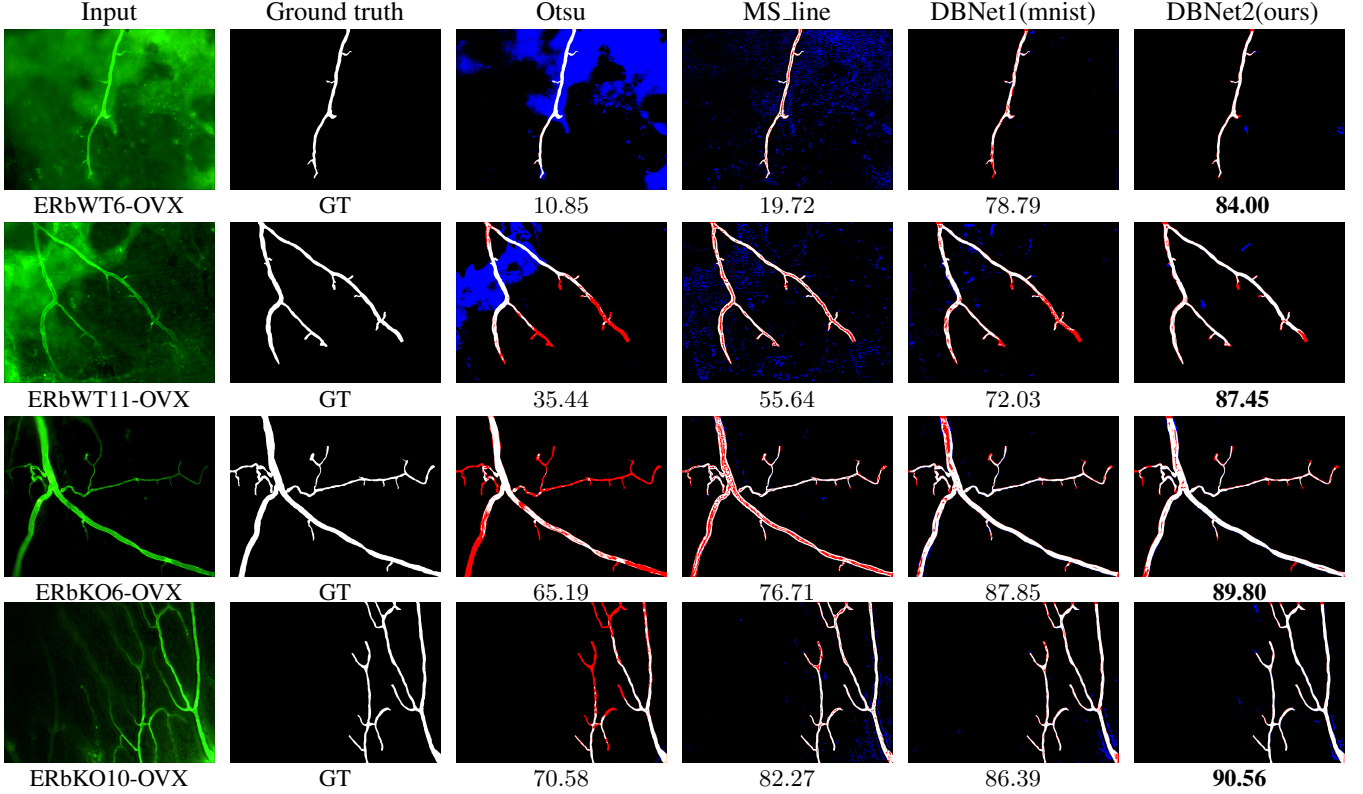


Fig. 5. Comparison of segmentation methods on (top to bottom) ER β -wild type (WT) images 6, 11, and ER β -knock-out (KO) images 6, 10. We show the optimal segmentation (with respect to the Dice metric) of different methods. (a) Input image, and (b) manually drawn ground truth (GT) of arterioles. Segmentation results obtained by (c) Otsu thresholding, (e) multiscale line detector (MS_line) [11], (f) deep network with 8 layers (DBNet1(mnist)), and (g) Our proposed deep network with 14 layers (DBNet2(ours)). White regions represent correctly segmented foreground pixels, red are missing (false negative) and blue are extra regions (false positive) compared to GT.

CNN framework proposed here obtains robust extraction of arterioles microvasculature networks.

3.2. Comparisons and Evaluations

Figure 4 shows comparison of Otsu thresholding, multiscale line detector (MS_line) from [11], and DBNet1(mnist) with our network DBNet2(ours). Table 2 compares the average Dice, sensitivity, specificity, and accuracy on a set of 20 epifluorescence microscopy OVX images. From Figure 5, we can see that Otsu thresholding obtains poor results while a state of the art segmentation method [11] got spurious segments and picked up a lot of background epifluorescence dye as foreground vessels. Further, the overall accuracy of [11] is less than that of our proposed CNN framework by 20% which confirms our images' complexity over retinal vessel segmentation problem. We also provide a comparison of another standard deep CNN (DBNet1(mnist)) from MatConvNet. We changed this network to be suitable for our two classes output requirement rather than ten, and trained it with patches equal to 28×28 . After training, the patches from the testing images will be provided to the network to get the final binary segmentation after reconstructing using all the overlapped patches.

As we can see, our adapted network obtained better results overall in all evaluation metrics. In particular, Otsu thresholding obtains the lowest values in both sensitivity and precision, while MS_line obtain lower precision, DBNet1(mnist) performs better than these two methods but obtained lower sensitivity and overall inferior to DBNet2(ours) performance.

4. CONCLUSIONS

In this paper, we considered the microvasculature segmentation with deep learning convolutional neural network (CNN) for challenging epifluorescence microscopy imagery. We proposed an architecture of CNN which is adapted to obtaining robust segmentation of microvasculature structures. By considering overlapping patches along with multiple convolutional layers, our method obtains good vessel differentiation for accurate segmentations. Experimental results showed that our proposed network obtained improved accuracy in segmentation over traditional approaches as well as a standard deep learning network. Further, our proposed CNN obtained good sensitivity, and precision when compared with traditional as well as a multiscale line detector based approach.

5. REFERENCES

- [1] S. Chaudhuri, S. Chatterjee, N. Katz, M. Nelson, and M. Goldbaum, “Detection of blood vessels in retinal images using two-dimensional matched filters,” *IEEE Trans. Med. Imag.*, vol. 8, no. 3, pp. 263–269, 1989.
- [2] A. F. Frangi, W. J. Niessen, K. L. Vincken, and M. A. Viergever, “Multiscale vessel enhancement filtering,” in *MICCAI*, 1998, pp. 130–137.
- [3] S. Cao, A. Bharath, K. Parker, J. Ng, J. Arnold, A. McGregor, and A. Hill, “Microvasculature segmentation of co-registered retinal angiogram sequences,” *Annals of British Machine Vision Association*, 2012.
- [4] V.B. Prasath, Y. M. Kassim, Z. A. Oraibi, J. B. Guiriec, A. Hafiane, G. Seetharaman, and K. Palaniappan, “Hep-2 cell classification and segmentation using motif texture patterns and spatial features with random forests,” in *IEEE ICPR*, 2016, pp. 90–95.
- [5] C. Panagiotakis and E. Kokinou, “Linear pattern detection of geological faults via a topology and shape optimization method,” *IEEE J. Sel. Topics Appl. Earth Observ. Remote Sens.*, vol. 8, no. 1, pp. 3–11, 2015.
- [6] S. Meena, V. B. S. Prasath, Y. M. Kassim, R. J. Maude, O. V. Glinskii, V. V. Glinsky, V. H. Huxley, and K. Palaniappan, “Multiquadrics based interactive segmentation of dura mater microvasculature from epifluorescence images,” in *IEEE EMBC*, 2016, pp. 5913–5916.
- [7] Y. M. Kassim, V. B. S. Prasath, R. Pelapur, O. Glinskii, R. J. Maude, V. Glinsky, V. Huxley, and K. Palaniappan, “Random forests for dura mater microvasculature segmentation using epifluorescence images,” in *IEEE EMBC*, 2016, pp. 2901–2904.
- [8] A. Sironi, E. Turetken, V. Lepetit, and P. Fua, “Multiscale centerline detection,” *IEEE Trans. Patt. Anal. Mach. Intell.*, 2015.
- [9] R. Pelapur, V. B. S. Prasath, F. Bunyak, O. Glinskii, V. Glinsky, V. Huxley, and K. Palaniappan, “Multi-focus image fusion on epifluorescence microscopy for robust vascular segmentation,” in *IEEE EMBC*, 2014, pp. 4735–4738.
- [10] V. B. S. Prasath, R. Pelapur, O. Glinskii, V. Glinsky, V. Huxley, and K. Palaniappan, “Multi-scale tensor anisotropic filtering of fluorescence microscopy for denoising microvasculature,” in *IEEE ISBI*, 2015, pp. 540–543.
- [11] U. T. V. Nguyen, A. Bhuiyan, L. A. F. Park, and K. Ramamohanarao, “An effective retinal blood vessel segmentation method using multi-scale line detection,” *Pattern Recognition*, vol. 46, no. 3, pp. 703–715, 2013.
- [12] J. Long, E. Shelhamer, and T. Darrell, “Fully convolutional networks for semantic segmentation,” in *IEEE CVPR*, 2015, pp. 3431–3440.
- [13] I. Goodfellow, Y. Bengio, and A. Courville, *Deep learning*, MIT Press, 2016.
- [14] O. Ronneberger, P. Fischer, and T. Brox, “U-Net: Convolutional networks for biomedical image segmentation,” in *MICCAI*, 2015, pp. 234–241.
- [15] D. C. Ciresan, A. Giusti, L. M. Gambardella, and J. Schmidhuber, “Mitosis detection in breast cancer histology images with deep neural networks,” in *MICCAI*, 2013, pp. 411–418.
- [16] H. Greenspan, B. van Ginneken, and R. M. Summers, “Deep learning in medical imaging: Overview and future promise of an exciting new technique,” *IEEE Trans. Medical Imag.*, vol. 35, no. 5, pp. 1153–1159, 2016.
- [17] K. K. Maninis, J. P. Tuset, P. Arbelaez, and L. V. Gool, “Deep retinal image understanding,” in *MICCAI*, 2016, pp. 140–148.
- [18] H.-C. Shin, H. R. Roth, M. Gao, L. Lu, Z. Xu, I. Nogues, J. Yao, D. Mollura, and R. M. Summers, “Deep convolutional neural networks for computer-aided detection: CNN architectures, dataset characteristics and transfer learning,” *IEEE Trans. Medical Imag.*, vol. 35, no. 5, pp. 1285–1298, 2016.
- [19] P. Teikari, M. Santos, C. Poon, and K. Hyynnen, “Deep learning convolutional networks for multiphoton microscopy vasculature segmentation,” *ArXiv 1606.02382*, 2016.
- [20] P. Liskowski and K. Krawiec, “Segmenting retinal blood vessels with deep neural networks,” *IEEE Trans. Medical Imag.*, vol. 35, no. 11, pp. 2369–2380, 2016.
- [21] A. Vedaldi and K. Lenc, “MatConvNet: Convolutional neural networks for MATLAB,” in *ACM Inter. Conf. Multi.*, 2015, pp. 689–692.
- [22] V. B. S. Prasath, F. Bunyak, O. Haddad, O. Glinskii, V. Glinskii, V. Huxley, and K. Palaniappan, “Robust filtering based segmentation and analysis of dura mater vessels using epifluorescence microscopy,” in *IEEE EMBC*, 2013, pp. 6055–6058.